OPEN ACCESS
IOP Publishing
Journal of Physics D: Applied Physics
J. Phys. D: Appl. Phys. 57 (2024) 405302 (9pp)
https://doi.org/10.1088/1361-6463/ad5c6f

Secondary electron emission yield in thick dielectric materials: a comparison between Kelvin probe and capacitive methods

R Mata[1,2,*], A Cros[2], B Gimeno[1,3] and D Raboso[4]

[1] Val Space Consortium, Ciudad Politécnica de la Innovación, Edificio 8G, Acceso B, Planta B, Camino de Vera s/n, 46022 Valencia, Spain
[2] Materials Science Institute (ICMUV). University of Valencia, C/Catedrático José Beltrán 2, Paterna, 46980 Valencia, Spain
[3] Instituto de Física Corpuscular, CSIC-University of Valencia, 46980 Valencia, Spain
[4] European Space Agency, ESTEC, Noordwijk, The Netherlands

E-mail: rafael.mata@uv.es

Received 12 February 2024, revised 11 May 2024
Accepted for publication 27 June 2024
Published 12 July 2024

Abstract

The recent high demand of secondary electron emission yield (SEY) measurements in dielectric materials from space industry has driven SEY laboratories to improve their facilities and measurement techniques. SEY determination by the common capacitive method, also known as pulsed method, is well accepted and has given satisfactory results in most cases. Nevertheless, the samples under study must be prepared according to the experimental limitations of the technique, i.e. they should be manufactured separated from the devices representing faithfully the surface state of the own device and be as thin as possible. A method based on the Kelvin probe (KP) is proposed here to obtain the SEY characteristics of electrically floating Platinum, Kapton and Teflon placed over dielectric spacers with thicknesses ranging from 1.6 to 12.1 mm. The results are compared with those of the capacitive method and indicate that KP SEY curves are less sensitive to spacer thickness. An explanation based on the literature is also given. In all, we have established that KP is better suited for the analysis of dielectric samples thicker than 3 mm.

Keywords: dielectrics, secondary electron emission yield, Multipactor in space devices

1. Introduction

Satellite communication devices use high power radio frequency (RF) signals operating under ultra-high vacuum. In these conditions, free (primary) electrons penetrating inside the component can be accelerated by the high electric fields present, eventually colliding against the component walls. Depending on their kinetic energy, primary electrons are expected to be either captured or backscattered, and their energy may be transferred to the electrons of the material, which might subsequently escape from the surface in a process known as secondary electron emission [1]. If during operation secondary electrons are then accelerated towards the opposite direction, an avalanche effect might break out, reflecting the RF and causing both: communication loss and a

* Author to whom any correspondence should be addressed.

potential damage of the components. This process is known as Multipactor Effect [2]. To prevent this undesirable RF breakdown, it is of paramount importance to characterize the secondary emission yield (SEY) of the materials involved in the manufacture of space RF components. The characterization technique is well-known and relatively easy to perform in good electrically conductive materials, since this property hinders surface charge accumulation. On the contrary, SEY measurements of dielectric materials has become a challenging process. Dielectrics might acquire positive or negative surface charge depending on the energy of the primary electrons. Therefore, it is mandatory to electrically neutralize the sample before the acquisition of each SEY curve. Otherwise, the charge accumulated at the sample surface will repel or attract the incident electrons, compromising the measurement. With the aim of avoiding the charging effect, the capacitive method is typically used, and the surface charge level is determined by indirect experimental calculations [3, 4], reducing the reliability of the results. Additionally, the main drawback of this method when applied to dielectrics is that it is only applicable to thin dielectric samples. Indeed, it may introduce considerable measurement errors if inappropriate sample geometries and thicknesses are used: the radiated front side and the pristine back of the sample act as a capacitor that interacts with the secondary electrons, changing the measured yield [5]. The Kelvin probe (KP) technique [6, 7], on the contrary, gives a measure of the surface voltage modified by the charging process. In this way, KP provides a direct verification of the presence of charge on the surface. Knowing the voltage variation, (ΔV), and the capacity (C) of the system, which can be experimentally determined by the same technique, the induced charge can be easily calculated ($Q = C\Delta V$).

In this paper, we study the SEY characteristics of Platinum, Kapton and Polytetrafluoroethylene (PTFE) placed over dielectric (Teflon) spacers of thicknesses ranging from 1.6 to 12.1 mm. The evolution of the SEY parameters obtained by the capacitive and KP methods are compared, analyzing the limitations and viability of the techniques.

2. Experimental setup and measurement methods

The facility used to develop this work is placed inside a 10.000 class (ISO 7) clean room with controlled temperature and humidity at the ESA-VSC High Power Space Materials Laboratory [8]. It was designed to measure the SEY characteristics of large samples and devices. In a vacuum chamber that reaches vacuum levels in the range of 10^{-8} mbar, two electron guns (e-guns) were installed to provide electron radiation in the energy range between 0 and 5000 eV in normal incidence. However, for this work SEY studies are restricted to energies between 0 and 2000 eV. The electron gun used in this study provides a Faraday cup, which is positively polarized at +59 V to measure dependably the primary current. The facility also provides a system composed by a Helium cold head and heating resistances that allows to vary the temperature between room temperature (∼23 °C). A Deuterium ultra-violet (UV) lamp (HAMAMATSU L15094) which provides photons with wavelengths from 115 to 400 nm is also installed and used for surface discharging. Finally, a KP system is also provided, and configured to work in vacuum, simultaneously with the e-gun.

As it was mentioned above, in this study SEY measurements were performed using two methods: common capacitive and KP. We will describe first the fundaments of the SEY capacitive method. In this case, due to the appearance of surface accumulation charge, when dealing with dielectric samples the current balance assumed in metallic samples cannot be applied. Accordingly, very small electron doses (∼10^7 electrons) are used to reduce charging effects. To measure the SEY coefficient properly, the following formula is used:

$$\mathrm{SEY} = \frac{Q_\sigma}{Q_\mathrm{p}} = 1 - \frac{Q_\mathrm{s}}{Q_\mathrm{p}}. \tag{1}$$

Here, Q_p represents the total primary charge obtained by time-integrating the incident current (primary pulses) measured using the Faraday cup and Q_σ is the charge produced by the secondary electrons. Q_s is the image charge obtained by time-integrating the current through the holder at the rear side of the sample, as indicated in figure 1(a). Since the primary charge equals the sum of Q_σ and Q_s, the equation can be reformulated as shown in the second expression of equation (1), containing easily measurable terms. These relations hold because the geometry of the sample allows to model it as a capacitor, formed between the upper and the lower sides of the material under analysis [5].

Regarding the KP method, the basic assumption considers that the surface potential will depend on the surface charge evolution, that is, the greater the number of emitted secondary electrons, the greater the induced variation in potential. This effect can be used to measure SEY by means of KP, as shown in detail in [9]. Considering that the sample forms a global capacitance C with the vacuum chamber, the trapped charge at the sample surface can be estimated by:

$$Q_t = C\Delta V(d) \tag{2}$$

where C will be later experimentally determined following the procedure explained in [9], and $\Delta V(d)$ is the difference surface potential before and after electron radiation which depends on the sample thickness d along the vertical direction (z-axis).

In ideal conditions, both KP and capacitive methods should be equivalent, that is, Q_s should be equal to Q_t. SEY can then be calculated as:

$$\mathrm{SEY} = 1 - \frac{Q_s}{Q_\mathrm{p}} = 1 - \frac{C\Delta V(d)}{Q_\mathrm{p}}. \tag{3}$$

However, values for Q_s and Q_t may be different, depending on the experimental and geometrical conditions, as shown in [6]. In the KP method, the equivalent capacitor to measure ΔV is formed between the KP tip and the irradiated zone. The

−150 °C and +300 °C. This study, however, is performed at distance between them can be maintained constant thanks to

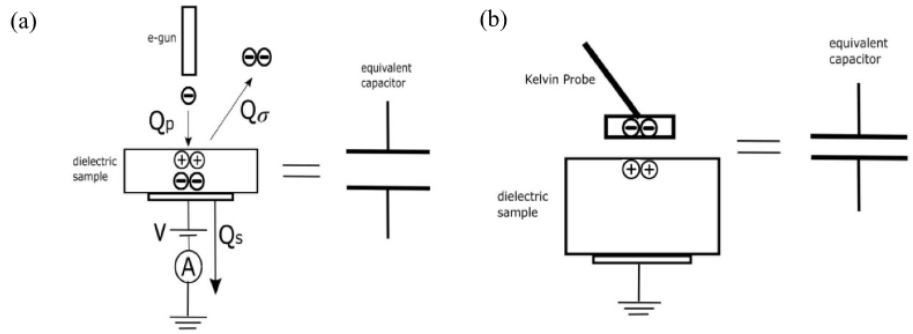

Figure 1. Equivalent capacitor formed in the capacitive (a) and the KP (b) methods for SEY measurements in dielectric materials.

the KP software, being therefore independent on the sample geometry, as it can be observed in figure 1(b).

The following general protocol was followed to reproduce SEY curves using both methods. (i) Each point of the SEY curve corresponds to a specific energy of the incident primary electrons (Ep). (ii) Before the sample is irradiated, it is discharged by applying UV radiation for two minutes while it is grounded. It was demonstrated by experimental measurements that two minutes was enough time to discharge the surface materials. This discharging procedure is equivalent to the second one explained in [10]. (iii) Each point was obtained by irradiating with a single primary electron pulse. (iv) While it is irradiated with the electron pulse, the sample is biased with a voltage of −29 V to avoid the recapture of secondary electrons. (v) Before proceeding with the next pulse, the sample is again grounded and illuminated with UV light with the aim of neutralizing again the surface charge.

Before and after the impact of each primary electron pulse, the surface potential ΔV was measured by means of KP. For each primary electron pulse, Q_s was also registered to reproduce the SEY coefficient using both expressions of equation (1). The inaccuracies of the measurements for the capacitive mode were estimated by obtaining experimental data from a reference sample consisting of an electrically contacted Platinum film. As a result, and considering the experimental dispersion at the maximum SEY signal, an error of 0.05 was assigned to the SEY coefficient. For the KP mode, the error propagation theory was applied to obtain a SEY error of 0.3. The energy error was estimated to be around 3 eV for all the SEY curves.

3. Sample design and characterization

Three thin (∼100 μm) samples of Platinum, PTFE, and Kapton were prepared in order to measure their SEY characteristics on four Teflon spacers of 1.6, 3.1, 6.1 and 12.1 mm thicknesses. PTFE and Teflon represent the same material. However, throughout this work we will refer to the sample as PTFE and to the spacer as Teflon. The spacers were chosen of Teflon due to its very low electrical conductivity [11] and negligible leakage currents when it is placed directly on a metallic electrode [12]. PTFE and Kapton were chosen considering their importance in space applications. For example, the multilayer insulators used to thermally protect the satellite made of Kapton, and a huge amount of wiring involved in satellites is covered with Teflon. Platinum is used as reference and was measured in two different modes: electrically contacted and isolated (floating). In this last configuration, the SEY from a metal can be measured using the KP method, which must give the same results than contacted since the SEY properties only depend on the surface state of the material. We used this characteristic to calibrate the SEY facility and verify the measurement methods. Additionally, this configuration simulates the floating metals in satellites due to the lack of grounding. Figures from 2(a) to (d) illustrate the detailed set-up for the Platinum sample electrically floating and placed over the different Teflon spacers. Figure 2(a) shows the electron gun (top) aligned with the KP (on the left) straight along the blue solid line. Sample and spacer are placed on a copper sample holder (bottom). The blue dashed line points to the axis of the copper holder.

The study started with the experimental determination of the capacitance C of each sample and spacer. However, since the contribution of the different samples is very small compared to the spacer, we will present only the results obtained for the floating Pt reference sample. For each spacer we followed five experimental steps, in a similar procedure as that illustrated in [7, 9]: (i) The sample on the spacer was placed in vacuum, grounded, and radiated with UV light for two minutes to neutralize the system. (ii) UV radiation was stopped, and the sample was biased with a potential of +56 V using battery supplied direct voltage to prevent electrons from escaping the surface. (iii) The surface voltage, V_i, was measured by KP. (iv) The sample was bombarded by a single electron pulse of 10 eV. This energy was chosen to provide a SEY lower than 1, which ensures the capture of all electrons. (v) Finally, KP was again used to measure the resulting surface voltage, V_f. The surface voltage variation $\Delta V = V_f - V_i$ was calculated and attributed to the injected charge. Steps from (i) to (v) were repeated several times, providing enough values of Q_s and ΔV

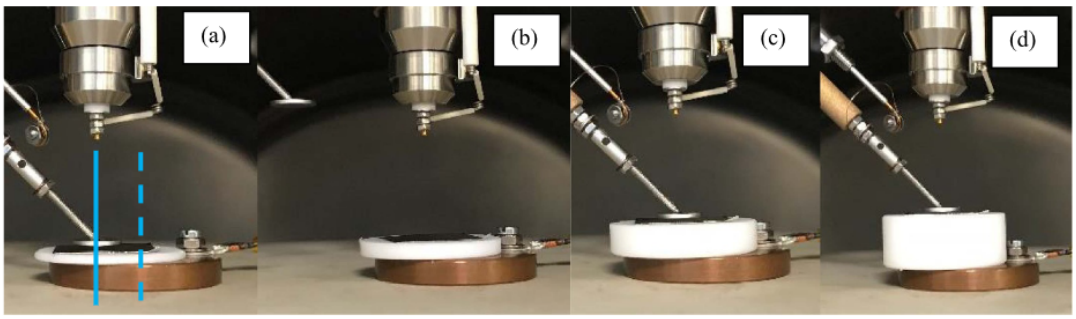

Figure 2. Floating Platinum sample over Teflon spacers of 1.6 (a), 3.1 (b), 6.1 (c) and 12.1 (d) mm thicknesses.

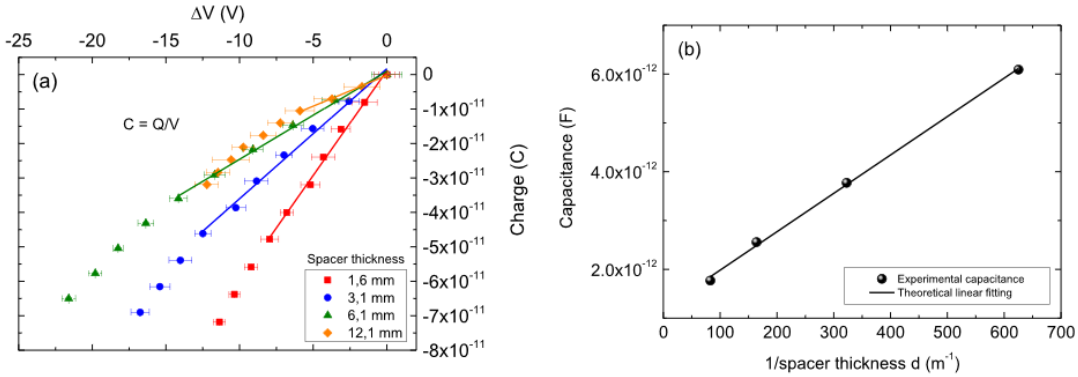

Figure 3. Capacitance determination as a function of spacer thickness: experimental points and linear fits (left); comparison between theoretical and experimental values of the capacitance as a function of the inverse of spacer thickness (right).

to extract the capacitance by a linear fit to equation (2). Finally, the injected charge dose was represented as a function of ΔV in figure 3(a). For the fitting, corresponding to the full lines in figure 3(a), only the points that follow a linear trend were used. This avoided deviations from the ideal planar capacitor induced by the electrostatic repulsion due to the large amount of trapped charge. Throughout this work, data represented with red squares, blue circles, green triangles, and orange diamonds will always be related to spacer thicknesses of 1.6, 3.1, 6.1, and 12.1 mm, respectively.

Black spheres in figure 3(b) show the measured capacitance as a function of the inverse of the spacer thickness. The theoretical capacitance was simulated by using the relation $C = \varepsilon_r \varepsilon_0 \frac{A}{d} + C_0$, where d is the sample thickness, A the surface radiated by the electron gun beam, C_0 is the parallel capacitance representing the contribution of the setup and, ε_0 and ε_r are the dielectric and the relative permittivity, respectively. As expected from a simple parallel plate capacitor model filled with Teflon ($\varepsilon_r = 2.1$), the results follow a linear trend compatible with a plate diameter of 23.2 $\pm$ 0.3 mm, which value is intermediate between the KP tip (15 mm) and the Teflon spacer diameters (30 mm). This discrepancy is attributed to edge effects that are not included in this theoretical model. Additionally, it is observed that the calculated capacitance is upward shifted by (1.20 $\pm$ 0.07) 10^{-12} F, indicating that the material samples are much thinner than the spacer, the contribution of the material samples to the whole capacitance was neglected. These experimental values follow the theoretical trend, confirming that the developed experimental process was properly designed.

As mentioned above, samples over different Teflon spacer thicknesses were biased with a potential of +56 V for the calculation of C, and with -29 V for SEY characterization. In both cases, this potential corresponds to the copper holder. Therefore, to determine properly the SEY curves, the real potential at the sample surface according to its variation along the vertical z-axis must be studied. For this purpose, each Teflon spacer was electrically neutralized by UV radiation and biased with -29 V. Afterwards, this potential was experimentally measured using the KP system for all the spacers and represented with black spheres in figure 4. Additionally, the potential distribution along the z-axis of a conductive disk was theoretically calculated and plotted in the same graph with a black line. The formula used for the simulation is: $V_{bias} = V_0(1 - z/\sqrt{R^2 + z^2})$ [14], where V_0 is the voltage at the conductive disk, R is the radius of the circular copper holder and z the distance parallel to the spacer thickness d. As it can be observed in figure 4, experimental results and theory follow the same trend with very close values. The discrepancies are attributed to charges that remain bounded to the spacer, which

ing that the electrical setup contributes to an additional parallel capacitance [13]. On the other hand, since the designed

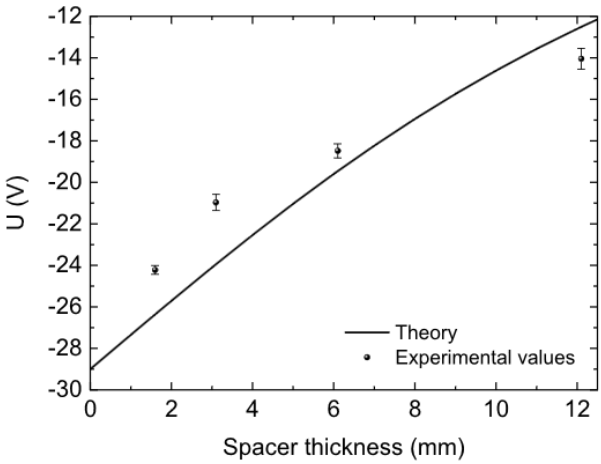

Figure 4. Bias potential applied for SEY acquisition as a function of the spacer thickness. Experimental values are represented with black spheres and theory with the curve.

calculated along the disk z-axis, while the experimental values were obtained off-axis (see figure 2(a) for visual clarification). Considering this agreement between experimental values and theory, the measured bias potential was used to shift the energy axis of the SEY curves.

4. Experimental results and discussion

SEY curves were obtained using both the capacitive and KP methods for all the samples over different dielectric spacers; SEY data are represented in figure 5. SEY curves from Platinum, Kapton and PTFE are shown in rows, respectively. The first column shows the capacitive method (empty symbols) and the right column the KP results (full symbols). Black dots refer to the electrically contacted Platinum sample used as reference. The dashed line indicates SEY $= 1$. Both methods were applied at the same time without changing the sample surface conditions between them. Therefore, the same generated charge at the material surface is evaluated by the capacitive and KP methods. Expectedly, the results should be the same. Nevertheless, significant differences were found.

Prior to the analysis of the results, it is important to consider that the samples used in this study were exposed to air and no special cleaning protocol was followed before the measurements. Considering that SEY characteristics strongly depend on surface conditions [15, 16], variations between our SEY values and previous studies [5, 17], where Platinum was cleaned by Ar^+ bombardment in vacuum, are expected. In this sense, our results are more similar to those obtained by Pintâo and Hessel, where they attributed that difference to the presence of possible impurities, such as an oxide layer on the platinum disk [18]. The effect of contaminants on the SEY of metals is well known, reducing the SEY once the surface is clean. However, the study of the SEY of dielectrics under are completely unknown, and to geometrical issues. In this sense, it is important to note that the theoretical voltage is in the literature. What is known is that in general terms the maximum SEY of contaminants is below 2.5. So it is expected that after atmospheric exposure dielectrics reduce their SEY [19]. Although, it has been observed that the SEY can increase from 2.4 [20] to 3.5 [21] when it is measured in fresh clean mica or exposed to air for a week, respectively. In our case, we encountered this trend for the dielectric materials involved in our investigation since they were exposed to atmospheric conditions for weeks. For example, Balcon *et al* [7] found a maximum SEY value of 1.7 for Kapton and a second cross over at 500 eV, while we obtain a value close to 2.4 and 1600 eV, respectively. Nevertheless, our results for the SEY maximum and second cross over for PTFE are close to their Teflon sample [7]. The same comparison can be found for Kapton and PTFE, respectively, in the compilation of experimental results elaborated by Cazaux [22]. These differences, however, are not relevant for the present study, focused mainly on the comparison between the capacitive and KP techniques for SEY acquisition, and the SEY variation with respect to the spacer thickness. In the case of the Platinum sample used as reference for capacitive and KP methods (black circles in figure 5), it must be highlighted that SEY curves acquired with the thinner spacer match very well with the reference (SEY from Pt electrically contacted) in both methods. This feature emphasizes that the SEY facility was properly optimized to avoid external disturbances in order to obtain accurate and representative SEY values. Although, it must be noted that SEY curves from Platinum obtained by KP method (graph in the first row and second column of figure 5) show a dispersion between them not observed in the rest of dielectric materials. We assume that this behavior is due to the error introduced by the charges located outside the KP tip area, since they redistribute in the whole Platinum surface due to its high electrical conductivity. However, this dispersion can be included in the SEY error obtained for the KP method.

First and foremost, it must be pointed out a remarkable result in figure 5 common for all the materials under analysis between the SEY when the SEY is close to its maximum value, obtained by capacitive (left column) and KP (right column) methods: the large variation of SEY curves obtained by the capacitive method when different spacer thicknesses are used, while a lack of this dependency is found in KP results. This variation is similar for all samples: SEY curves decrease as the dielectric spacer thickness increases. According to many works [4, 23, 24], it has been demonstrated that in dielectrics, the positive generated charge by primary electrons when SEY > 1 is generated in the range of few nanometres far from the material surface. Simultaneously, the image charge is produced at the opposite sample surface influenced by the generated potential at the irradiated surface, which has an inverse dependence with the distance. This behavior reflects the fact that the detected image charge at the rear side of the sample by the capacitive method and the induced charge at the irradiated side are not the same. The influence of the spacer is especially noticeable for thicknesses above 3 mm, introducing a significant error in the SEY results obtained by the capa-

the influence of contaminants at the surface is extremely poor

citive method. In agreement with the fact that for thin films

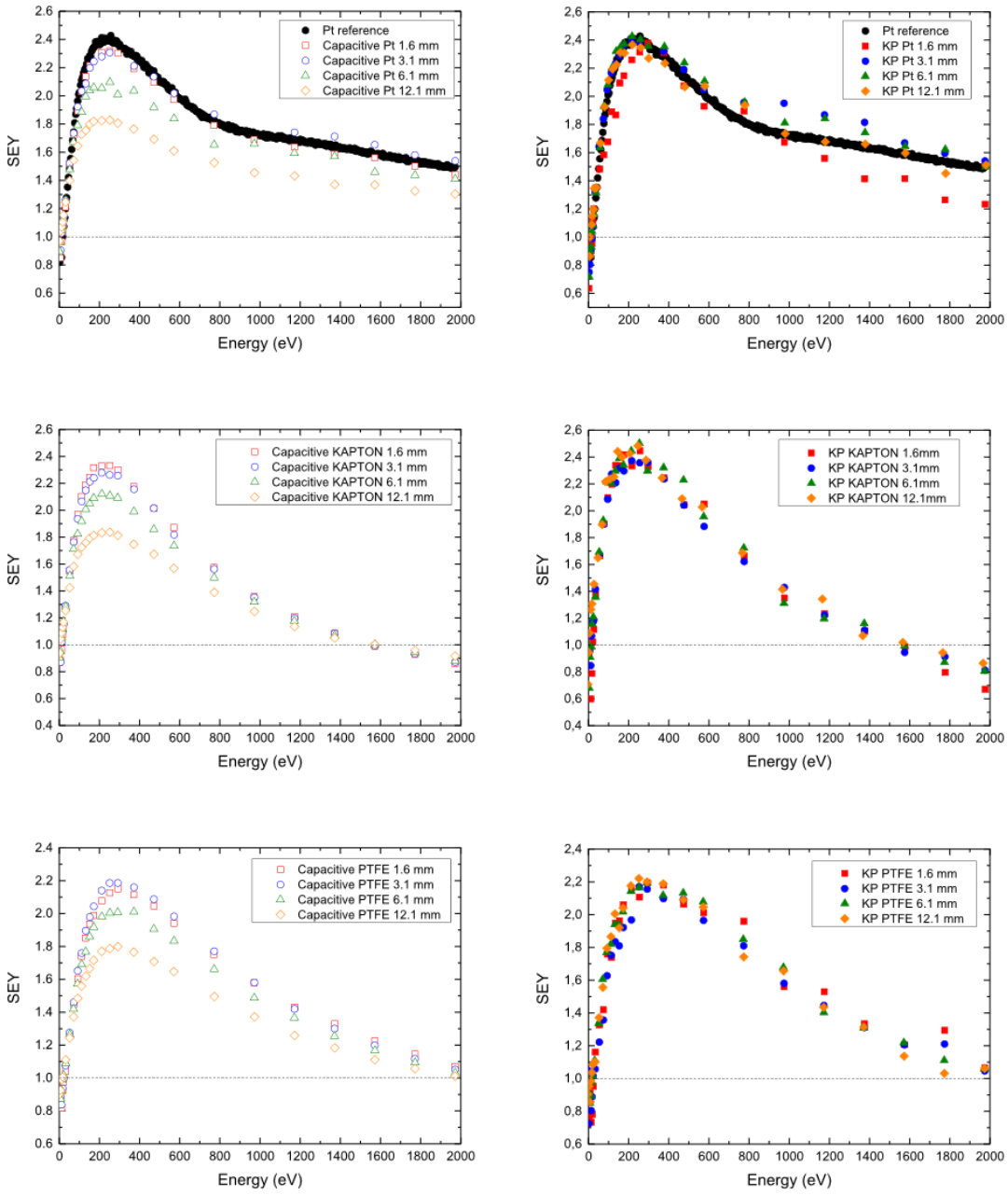

Figure 5. SEY curves from Pt electrically floating (first row), Kapton (second row), and PTFE (third row) measured using the capacitive (left column) and KP (right column) methods.

the capacitance increases, leading to a lower surface potential and therefore reducing the potential barrier and minimizing the error associated to the capability of low energy electrons to escape from the surface [3, 25]. According to the capacitor formed between both sides of the sample sketched in figure 1(a), this effect is absent in KP measurements since this method directly provides the surface potential induced by the generated charge at the irradiated sample surface. Therefore, the SEY measurement is not influenced by the dielectric spacer thickness according to the formed capacitor shown schematically in figure 1(b). On the other hand, it is observed that SEY curves obtained by capacitive (empty symbols) and KP (full symbols) methods are very similar for the two thinnest spacers (1.6 and 3.1 mm) for all the materials (red squares and blue circles). Additionally, it is noticeable how all the SEY curves obtained for all the spacers by the capacitive method both for

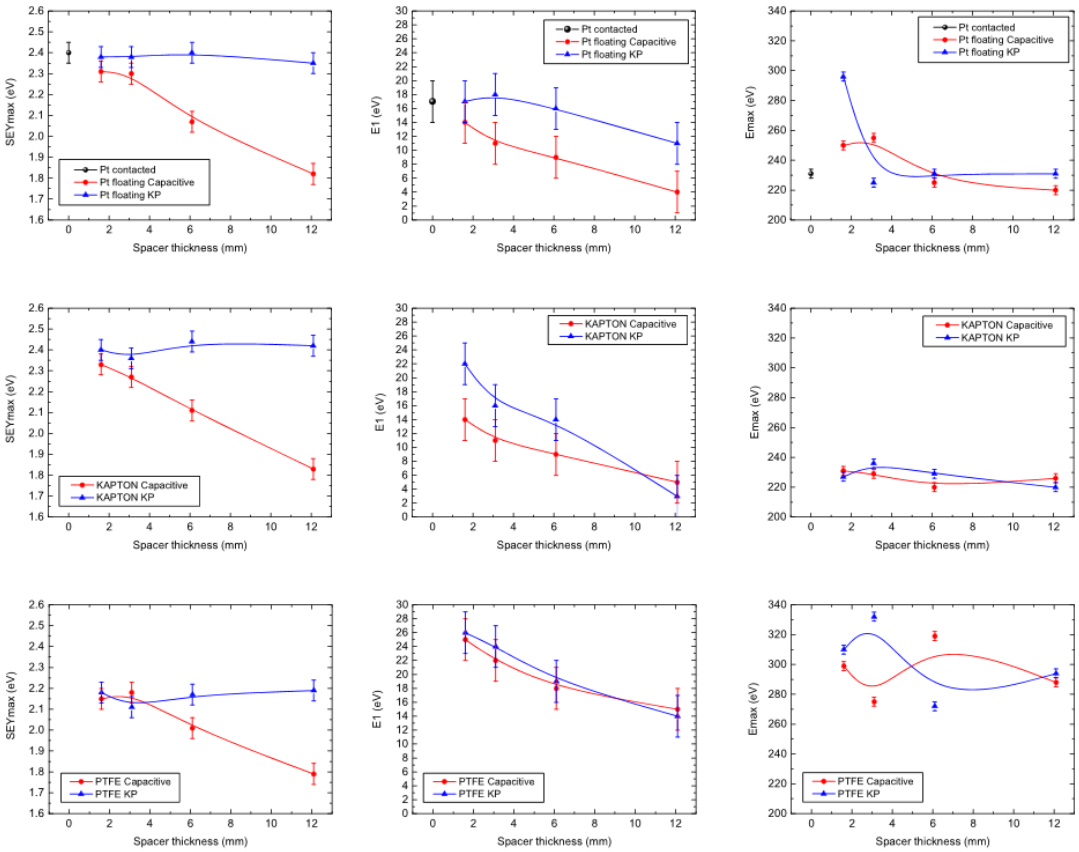

Figure 6. SEYmax (first column), E1 (second column), and Emax (third column) parameters for Platinum (first row), Kapton (second row), and PTFE (third row) as a function of the spacer thickness.

Kapton and PTFE converge as the primary energy increases. This behavior is found for both materials SEY curves and it was explained by Hessel and Gross [4] assuming that electrons undergoing emission recombine with holes stored in the surface layer of the dielectric and because the positive charge volume generated inside the material moves away from the surface to larger depths beyond the scape depths of secondary electrons.

The main SEY parameters (maximum secondary electron emission yield coefficient, SEYmax; its corresponding energy, Emax; and the first cross-over, E1, for SEY = 1) were extracted from all the curves and plotted in columns in figure 6 as a function of spacer thickness. To obtain these parameters, polynomial fits were used in the regions of E1 and Emax. Values from the electrically contacted Pt reference sample are represented in black spheres. Results from the capacitive method are plotted in red circles, while parameters from KP method are represented with blue triangles. Each row of graphs corresponds to Platinum, Kapton and PTFE, respectively, while the parameters are organized in columns: SEYmax, E1 and Emax from left to right, respectively.

This representation using the SEYmax parameter (left column of figure 6) clearly shows the aforementioned variation (red circles) for all the materials under study if it is applied on samples thicker than 3 mm. As expected, this SEYmax tendency is not observed using the KP method (blue triangles), which agrees with the fact that SEY parameters depend only on the material surface properties and not on the measure technique applied. Additionally, it must be pointed out that for Platinum, all the values obtained by KP method remain constant at the SEYmax reference one. This finding is considered of utmost importance since it allows to quantify the maximum sample thickness to obtain reliable SEY results in non-conductive materials if the capacitive method is used. Otherwise, other techniques, such as KP must be considered.

Regarding the first cross-over results, E1, these are represented in the middle column of figure 6 for Platinum, Kapton and PTFE, respectively. As it can be clearly observed for all the materials, E1 extracted from SEY curves obtained by the capacitive method (red circles) continuously decreases as the spacer thickness increases. This behavior is a consequence of the direct application of the sample bias potential, as it is commonly performed, whereas for thicker samples the potential decreases according to figure 4, underestimating in consequence the real values. Therefore, with the aim of obtaining realistic results, all the SEY curves have been energetic-

column of figure 6) clearly shows the aforementioned variation of the SEY curves in values obtained by the capacitive method ing realistic results, all the SEY curves have been energetically shifted using the real potential at the irradiated sample

surface measured by KP (experimental values of figure 4) for the corresponding spacer thickness. The results are plotted with blue triangles in the same charts of figure 6. As expected, Platinum shows a constant value of E1 equal to the reference one for all the spacers thicknesses except for the thickest one, whose value slightly decreases. However, E1 values from Kapton and PTFE unexpectedly show the same trend than for those obtained by the capacitive method: continuously decreasing as the spacer thickness increases. Although, it should be noticed that for the same spacer thicknesses, the energetic delta between E1 values obtained from capacitive and KP methods decreases further from Platinum, Kapton and PTFE, sequentially. In the last two cases, inverting its position for the thickest spacer. All these features are consistent with the presence of a remaining positive charge at the sample surface that is more difficult to neutralize by electron recombination as the conductivity of the material decreases, being up to three orders of magnitude in PTFE compared to Kapton [11, 26].

Finally, concerning the Emax parameter, it is found a lack of dependency on the spacer thickness for all the materials studied in this work. However, it can be mentioned the higher dispersion ($\pm$40 eV) observed in the values obtained from PTFE, while for Kapton the dispersion is lower ($\pm$20 eV). This feature, is also in agreement with the presence of a remaining layer of charges at the sample surface, being more remarkable this shift around the SEYmax region. Hoffman *et al* [24] shows that due to the positive potential produced by the secondary electrons that reach the surface when SEY $>$ 1, some of them can be reattracted forming a shallow negative layer. Both positive and negative regions are found in the length of the escape depth. Therefore, depending on their balance, it might shift the SEY curve in both energetic directions given a higher and lower dispersion depending on the material conductivity.

In summary, and considering all the aforementioned findings, we consider that these results demonstrate the utmost importance of both the proper sample design and the suitable technique of analysis to obtain reliable SEY results according to the nature (dielectric) and geometry of the samples.

5. Conclusions

The acquisition of SEY curves in dielectric materials requires a complex set-up and procedures. In this study, we have evaluated an alternative measuring method to provide more reliable results in bulky dielectric materials. For this purpose, a KP system was installed in a vacuum chamber to work in combination with an electron gun to measure the SEY properties from dielectric materials and compare the results with the commonly used capacitive method. To evaluate the response of both techniques in thick dielectrics, several Teflon spacers were designed and manufactured to measure the SEY from Platinum electrically isolated, Kapton and PTFE. The SEY from the electrically contacted Platinum sample was also measured and used as reference. It was found that using the the dielectric spacer thicknesses, in agreement with the fact that SEY properties should only depend on material surface characteristics, and not on its geometry. On the contrary, it is found out that this parameter decreases as the spacer thickness increases, if it is measured using the capacitive method, because of the underestimation of the measured image current at the rear side of the sample. Therefore, it has been demonstrated that 3 mm thickness seems to be the maximum dimension in dielectric materials to obtain reliable results using the capacitive method. The KP method is better suited for thicker samples. In addition, it is observed that E1 parameter obtained by capacitive method decreases with the spacer thickness for all the materials involved in this study as a consequence of applying the bias potential at the metallic sample holder for the SEY energetic shifting. The real potential at the irradiated sample surface was measured by KP and applied for the SEY curve energetic shifting. It is found that E1 parameter for Platinum remains constant for all the spacers except of the thickest one, whose value slightly decreases. However, E1 from Kapton and PTFE unexpectedly follows the same trend for both techniques: decreasing as the spacer thickness increases. Finally, it was expected to find a relative constant value of Emax for all the spacer thicknesses measured by both methods in all the materials. Nevertheless, a considerable dispersion was found. Features related to E1 and Emax suggest that they are influenced by the presence of a layer of charges at the sample surface, being more remarkable these effects for materials with lower electrical conductivity. The findings of this work encourage the use of suitable techniques for SEY analysis depending on the nature and geometry of the samples.

Data availability statement

All data that support the findings of this study are included within the article (and any supplementary files).

Acknowledgments

The authors would like to thank the ESA/VSC European High Power Space Materials Laboratory for its contribution—a laboratory funded by the European Regional Development Fund—a way of making Europe. And, to the European Space Agency for the given support and funding through the research activity VSC/2022/R&D/ESA/KP/1. A C acknowledges funding from Generalitat Valenciana through project CIPROM-2021-75 and from the Advanced Materials programme supported by MCIN with funding from European Union NextGenerationEU (PRTR-C17.I1) and by Generalitat Valenciana; Grant MFA/2022/007.

ORCID iDs

R Mata https://orcid.org/0000-0001-7087-3796

KP method, the SEYmax parameter remains constant for all

A Cros https://orcid.org/0000-0002-8264-3311

References

[1] Scholtz J J, Dijkkamp D and Schmitz R W A 1996 Secondary electron emission properties *Philips J. Res.* **50** 375–89

[2] de Lara J, Perez F, Alfonseca M, Galan L, Montero I, Roman E and Garcia-Baquero D R 2006 Multipactor prediction for on-board spacecraft RF equipment with the MEST software tool *IEEE Trans. Plasma Sci.* **34** 476–84

[3] Gross B and Hessel R 1991 Electron emission from electron-irradiated dielectrics *IEEE Trans. Dielectr. Electr. Insul.* **26** 18–25

[4] Hessel R and Gross B 1992 Escape depth of secondary electrons from electron-irradiated polymers *IEEE Trans. Dielectr. Electr. Insul.* **27** 831–4

[5] Bañón-Caballero D *et al* 2018 Study of the secondary electron yield in dielectrics using equivalent circuital models *IEEE Trans. Plasma Sci.* **46** 859–67

[6] Belhaj M, Tondu T, Inguimbert V, Elsafi B, Fakhfakh S and Jbara O 2012 Electron emission yield and charging process of alkali-silicate glass submitted to an electron beam under the varying temperature condition *Nucl. Instrum. Methods Phys. Res.* B **270** 120–7

[7] Balcon N, Payan D, Belhaj M, Tondu T and Inguimbert V 2012 Secondary electron emission on space materials: evaluation of the total secondary electron yield from surface potential measurements *IEEE Trans. Plasma Sci.* **40** 282–90

[8] Val Space Consortium 2011 (available at: www.val-space.com/en/esa-vsc-european-high-power-space-materials-laboratory/)

[9] Tondu T, Belhaj M and Inguimbert V 2010 Methods for measurement of electron emission yield under low energy electron-irradiation by collector method and Kelvin probe method *J. Vac. Sci. Technol.* A **28** 1122–5

[10] Belhaj M, Tondu T and Inguimbert V 2009 Experimental investigation of the effect of the internal space charge accumulation on the electron emission yield of insulators submitted to e-irradiation: application to polycrystalline MgO *J. Phys. D: Appl. Phys.* **42** 145306

[11] Nishi Y, Iizuka S, Faudree M C and Oyama R 2012 Electrical conductivity enhancement of PTFE (Teflon) induced by homogeneous low voltage electron beam irradiation (HLEBI) *Mater. Trans.* **53** 940–5

[12] Yuan L, Zheng X, Zhu W, Wang B, Chen Y and Xing Y 2024 Study on the electrical insulation properties of modified ptfe at high temperatures *Polymers* **16** 316

[13] Grove T T, Masters M F and Miers R E 2005 Determining dielectric constants using a parallel plate capacitor *Am. J. Phys.* **73** 52–56

[14] Jackson J D 1962 *Classical Electrodynamics* 1st edn (Wiley)

[15] Montero I, Olano L, Aguilera L, Dávila M E, Wochner U, Raboso D and Martín-Iglesias P 2020 Low-secondary electron emission yield under electron bombardment of microstructured surfaces, looking for multipactor effect suppression *J. Electron Spectrosc. Relat. Phenomena* **241** 146822

[16] Nistor V, González L A, Aguilera L, Montero I, Galán L, Wochner U and Raboso D 2014 Multipactor suppression by micro-structured gold/silver coatings for space applications *Appl. Surf. Sci.* **315** 445–53

[17] Bronchalo E, Coves Á, Mata R, Gimeno B, Montero I, Galán L, Boria V E, Mercadé L and Sanchís-Kilders E 2016 Secondary electron emission of pt: experimental study and comparison with models in the multipactor energy range *IEEE Trans. Electron Devices* **63** 3270–7

[18] Pintâo C A F and Hessel R 2000 Total secondary-electron yield of metals measured by a dynamic method *J. Appl. Phys.* **88** 478

[19] Barnard J, Bojko I and Hilleret N 2023 Measurements of the secondary electron emission of some insulators (arXiv:1302.2333v1)

[20] Seiler H 1983 Secondary electron emission in the scanning electron microscope *J. Appl. Phys.* **54** R1–8

[21] Hopman H J, Alberda H, Attema I, Zeijlemaker H and Verhoeven J 2003 Measuring the secondary electron emission characteristic of insulators *J. Electron Spectrosc. Relat. Phenomena* **131–132** 51–60

[22] Cazaux J 2005 A new model of dependence of secondary electron emission yield on primary electron energy for application to polymers *J. Phys. D: Appl. Phys.* **38** 2433–41

[23] Ganachaud J P and Mokrani A 1995 Theoretical study of the secondary electron emission of insulating targets *Surf. Sci.* **334** 329–41

[24] Hoffmann R, Dennison J R, Thomson C D and Albretsen J 2008 Low-fluence electron yields of highly insulating materials *IEEE Trans. Plasma Sci.* **36** 2238–45

[25] Scholtz J J, Schmitz R W A, Hendriks B H W and de Zwart S T 1997 Description of the influence of charging on the measurement of the secondary electron yield of MgO *Appl. Surf. Sci.* **111** 259–64

[26] Kapton HN (available at: www.dupont.com/products/kapton-hn.html) (Accessed 8 July 2020)